nature communications

Article

https://doi.org/10.1038/s41467-025-60270-x

Pd/C promotes C–H bond activation and oxidation of *p*-hydroxybenzoate during hydrogenolysis of poplar

Received: 16 December 2024

Accepted: 19 May 2025

Published online: 06 June 2025

Check for updates

Canan Sener[1,2], Vitaliy I. Timokhin[1,2], Jan Hellinger[1,2], John Ralph[1,2,3] & Steven D. Karlen[1,2]

Hydrogenolysis of lignin generates a portfolio of products, the yields of which are generally calculated using a subset of phenolic monomers that are dependent on the lignin composition, product distribution, and analytical technique. Some lignins are naturally γ-acylated; poplar lignins, for example, have *p*-hydroxybenzoate groups on 1–15% of their syringyl subunits. Upon hydrogenolysis, it is generally assumed that the *p*-hydroxybenzoate is cleaved before the deacylated lignin is depolymerized. Hydrogenolysis of model γ-*p*-hydroxybenzoylated β-aryl ethers do not, however, produce the deacylated β-aryl ether intermediates, as was previously conjectured; products instead derive from palladium-assisted reactions on the cinnamyl *p*-hydroxybenzoates resulting in initial β-ether cleavage. The *p*-hydroxybenzoate moiety itself also undergoes carboxylate-assisted palladium-catalyzed C–H bond activation to form the 2,4-dihydroxybenzoate, that subsequently converts to the 2,4-dihydroxycyclohex-1-enoate. These details underscore previously unrecognized pathways and products that are key to understanding the different hydrogenolysis product distributions from naturally acylated lignins that are prevalent biomass-conversion feedstocks.

Hydrogenolysis of lignocellulosic biomass depolymerizes the lignin component into a hydrogenolysis oil comprised of small lignin monomers, dimers, and higher oligomers. The chemical composition of the produced oil is directly related to the reaction conditions (i.e., catalyst, biomass-to-solvent loading, solvent, pressure, temperature, reaction time) and the feedstock used[1,2]. Research efforts to optimize hydrogenolysis conditions primarily target the cleavage of β-aryl ethers, as these are the most abundant interunit linkages accounting for ~60% of the lignin. The other common units: resinol (β-β), phenylcoumaran (β–5), and biphenyl (5-5) are C–C-bonded and are much harder to cleave, whereas the 4-*O*-5 units contain phenolic ethers that can be cleaved by hydrogenolysis[3] but are typically minor components. Focusing on the β-aryl ethers, there are several key bonds of interest to cleave. These are, in increasing bond-strength order, C_α–OH < C_β–OAr < C_α–C_β < C_α–C_1[4,5]. As a benzylic alcohol, the C_α–OH bond is the weakest bond due to the stabilization of any incipient carbonium ion provided by the adjacent electron-rich aromatic ring and readily undergoes dissociation. The second weakest bond is the C_β–OAr that, under homolysis, forms the monolignols, Hibbert's ketones, formaldehyde, and/or other products.

Under mild processing conditions, the products are phenolic monomers that retain the aromaticity of the phenyl rings, as well as the methoxy groups found on the 3-position of the guaiacyl (G) units and the 3,5-positions of syringyl (S) units. When the catalyst is palladium-based (e.g., Pd/C), the major phenolic monomers are arylpropanol products **1**, whereas the arylpropane products **2** and compounds with truncated sidechains (no sidechain **3**, methyl **4**, and ethyl **5**) are minor products (<10% of the monomers), Fig. 1. In the absence of catalyst, the product distribution reflects low temperature (≤200 °C) acid-catalyzed decomposition products that are characterized by

[1]Wisconsin Energy Institute, University of Wisconsin, Madison, WI, USA. [2]DOE Great Lakes Bioenergy Research Center, University of Wisconsin, Madison, WI, USA. [3]Department of Biochemistry, University of Wisconsin, Madison, WI, USA. e-mail: skarlen@wisc.edu

https://doi.org/10.1038/s41467-025-60270-x

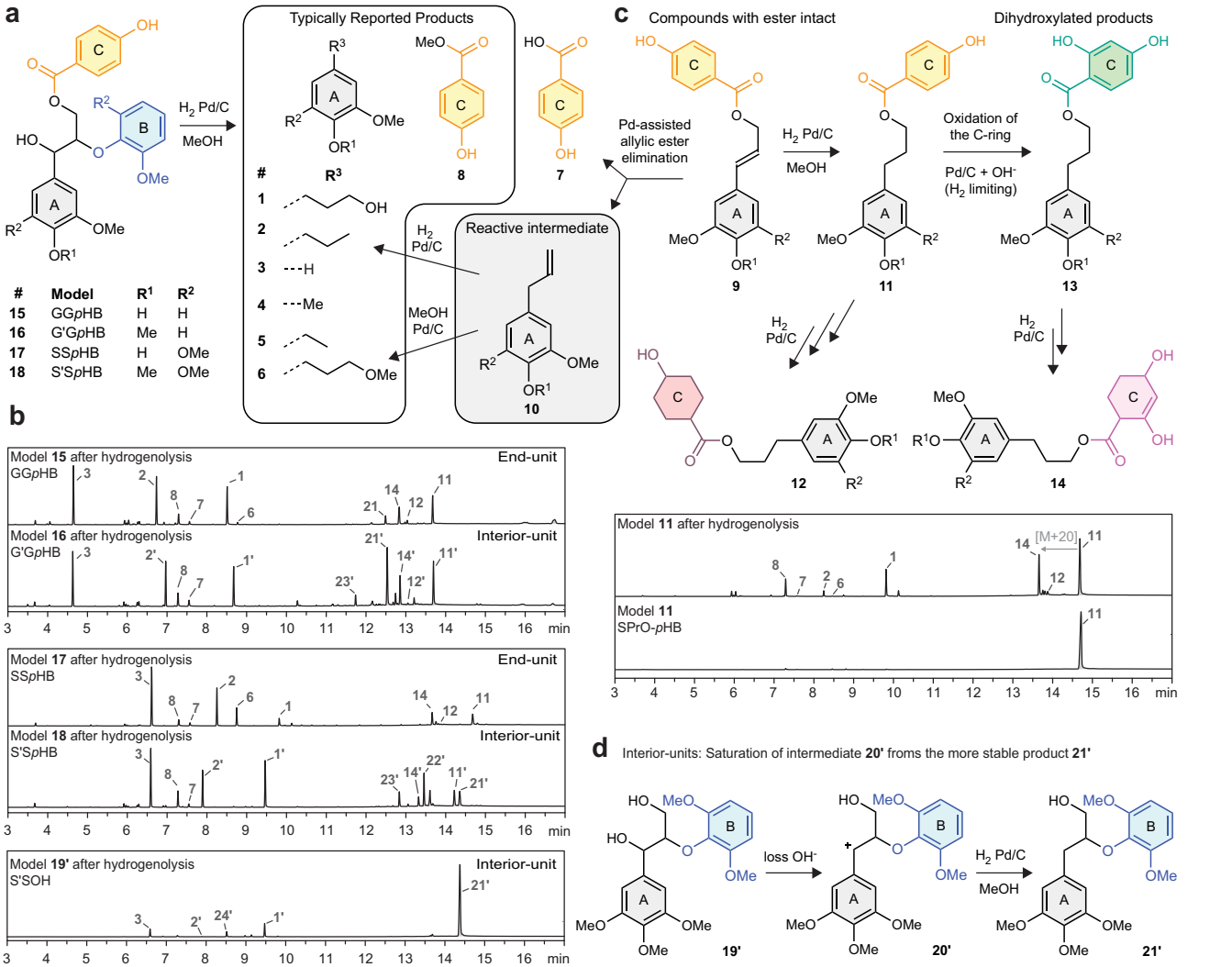

Fig. 1 | Hydrogenolysis of β-*O*-4 subunits with and without γ-acylation forms an array of phenolic monomer products (compounds 1 – 14). a Model compounds **15** and **17** represent γ-*p*HB-acylated β-ether end-units (free-phenolic) and compounds **16** and **18** represent the analogous internal subunits that are 4-*O*-etherified. Hydrogenolysis of **15**–**18** produces phenolic monomers **1**–**8** and phenolic conjugates **11**, which retain the γ-*p*-hydroxybenzoate. **b** GC-MS chromatograms of the hydrogenolysis products from compounds **15**–**18**. **c** Hydrogenolysis of compound **11** produced previously unknown ester products **12**–**14**, with the primary products being **14**, **1**, and **8**. **d** Hydrogenolysis of compound **19'** shows a strong signal for the arylpropanol **1'** and stabilized product **21'**. Primary monolignol A-ring and sidechain in the model compounds **15**-**18** are in black, with β-ether B-ring in blue, and the γ-*p*HB in yellow. The products formed from these subunits keep their color, with the exception of the γ-*p*HB, which becomes red when saturated (**12**), green when oxidized (**13**), and pink when both oxidized and partially saturated (**14**).

homolysis of terminal 4-hydroxy end-units, regeneration the monolignols, formation of Hibbert's ketones, and the release of formaldehyde that results in the formation of truncated sidechains (no sidechain **3**, methyl **4**, and ethyl **5**) and condensation products[6–8]. In the hydrogenolysis of biomass, the major monophenolic products are compounds **1** and **2** with a typical ratio of ~90:10 for softwoods (conifers) that have guaiacyl/4-hydroxyphenyl (G/H) lignins, and most hardwoods (e.g., maple, beech, and eucalyptus) that have syringyl/guaiacyl (S/G) lignins. Various γ-acylated lignins are produced in many clades of angiosperms (flowering plants). Hydrogenolysis of biomass from these species results in higher levels of arylpropanes **2** than observed from non-acylated lignins. Two of the most studied clades in biomass conversion, the commelinid monocots (e.g., grasses, sedges, and palms) and the Salicaceae family (e.g., poplar and willow), both have naturally acylated lignins[9–13]. Delineating the hydrogenolytic pathways of acylated lignin units, therefore, becomes important for understanding the variations in the **1**:**2** ratios.

The Salicaceae family of hardwoods (*Populus* and *Salix*) produce lignins with *p*-hydroxybenzoate pendent groups acylating the γ-hydroxyl of the lignin sidechains, predominantly on S-units[9,14]. The *p*-hydroxybenzoate content ranges from 0.5–2.9 wt% of the biomass[15]. It is now well established that such acylated lignin units, like their earlier-determined acetate[16,17] and *p*-coumarate analogs[18–20], derive from lignification using pre-acylated monolignols, coniferyl and sinapyl *p*-hydroxybenzoate **9** in this case[14,21,22]. Lignin depolymerization by hydrogenolysis of these γ-acylated lignins requires three reactions to occur in order to cleave the β-aryl ether (henceforth termed simply "β-ether") units and generate arylpropanol **1** and methyl *p*-hydroxybenzoate **8** from the pendent group (when the hydrogenolysis is conducted in methanol and the γ-acylating unit is *p*-hydroxybenzoate, *p*HB). (1) The *p*HB group needs to be released and converted to its methyl ester. This is achieved either directly by transesterification or through hydrolysis followed by esterification, (2) The hydroxy group on the α-carbon of the β-ether needs to be replaced with a hydrogen, and (3) The β-ether bond needs to be broken and with another hydrogen replacement.

Herein, we show how the presence of a γ-acyl group alters the product portfolio produced by hydrogenolysis with Pd/C as the

heterogenous catalyst. We synthesized a family of β-ether model compounds **15**–**18** in which the γ-OH was acylated with *p*-hydroxybenzoate, Fig. 1. The product distribution after hydrogenolysis of these esters shows that depolymerization starts by cleavage of the β-aryl ether bond, to form the arylpropenyl esters **9** that are subsequently converted to arylpropyl esters **11**, ethers **6**, the arylpropanols **1**, the arylpropanes **2**, *p*-hydroxybenzoic acid **7**, or methyl *p*-hydroxybenzoate **8**. Additionally, the *p*-hydroxybenzoate unit in ester **11** underwent both reduction to 4-hydroxycyclohexanoate **12** and oxidation via carboxylate-assisted palladium-catalyzed C–H bond activation to the 2,4-dihydroxybenzoate ester **13**, which is subsequently reduced to the 2,4-dihydroxycyclohex-1-enoate ester **14**. As the time-course study of hydrogenolysis of poplar presented in Fig. 2 shows, when γ-acyl groups are present in the lignin, the generally quantified set of phenolic monomers is missing a significant portion of the lignin depolymerization products.

Results

Hydrogenolysis of γ-acylated β-ether models

Lignin end-unit models **15** and **17**, Fig. 1, are characterized by a 4-OH on the primary "A-ring." The 4-hydroxy group provides resonance stabilization to benzylic cations and, through loss of the acidic 4–OH proton, can form a quinone methide structure. This is in contrast with internal lignin subunits that are 4-*O*-etherified (i.e., 4-*O*-β, 4-*O*-5, and 4-*O*-α/β-5) that, although they still provide resonance stabilization to a benzylic cation, lack the acidic proton. These internal β-aryl ethers

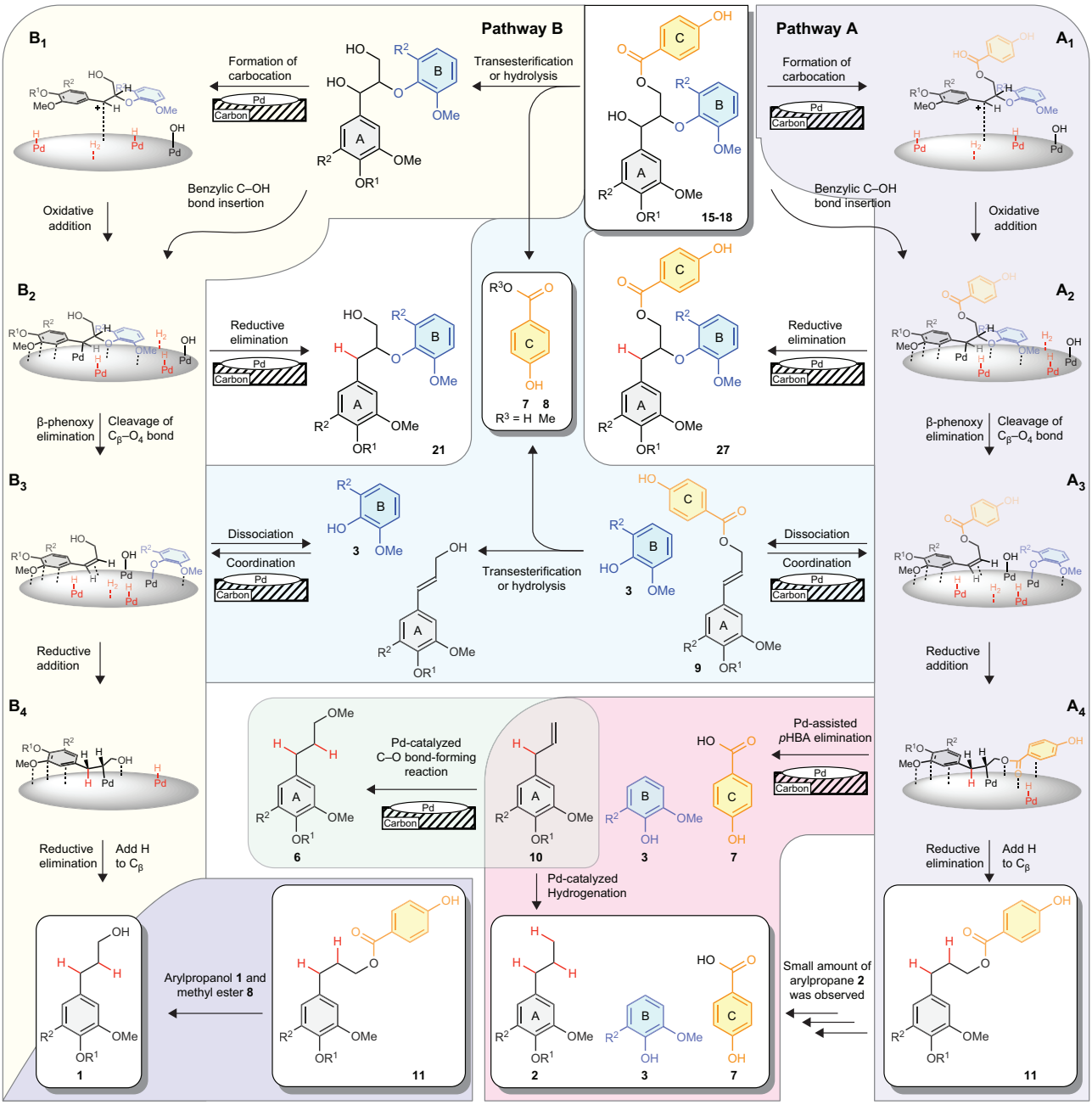

Fig. 2 | Reaction pathways for the hydrogenolysis of β-ether units with and without γ-acylation by *p*-hydroxybenzoate. The formation of product **11** is only possible when β-ether cleavage is faster (pathway A) than either hydrolysis or transesterification of the conjugate (pathway B). Only pathway A can produce all the observed products. Primary monolignol A ring and sidechain in the model compounds **15**-**18** are in black, the β-ether B-ring is in blue, the γ-*p*HB is in yellow, and the added hydrogens are in red.

units are well-modeled by 4-*O*-methylation of the primary "A-ring" phenol in models **16** and **18**; 4-OMe monomer products from these models will be denoted in the figures with a prime in the compound abbreviations (e.g., **1′** and **2′**). The γ-*p*-hydroxybenzoylated β-ether model compounds **15**–**18** were subjected to hydrogenolysis in MeOH with Pd/C for 180 min at 200 °C, resulting in conversion of the majority of the substrate to a distribution of products, Fig. 1 and Supplementary Tables 3–6. The major products were a mixture of arylpropanol **1** and arylpropane **2** monomers from the core-lignin moiety, the β-ether cleavage product **3** that has no sidechain due to the limitations of the model, and a series of higher-molecular-weight products. These results indicate that hydrogenolysis of γ-acylated β-ethers **15**–**18** form arylpropane monomers **2** more efficiently than, or as efficiently as, they form arylpropanol monomers **1**, Fig. 1b (top two panels). This contrasts with non-acylated γ-hydroxy-β-ether model compounds that form arylpropanols **1** with substantially higher preference, Fig. 1c and Supplementary Table 7[23,24]. When the A-ring phenol is methylated (e.g., compound **19′** in Fig. 1e), hydrogenation of the carbocation **20′** to the stable α,β-saturated product **21′** is faster than β-ether cleavage[23]. In all cases, the presence of compounds **11** and **11′** in the product mixture from γ-acylated β-ether models **15**–**18**, suggests that the reaction pathway proceeds via cleavage of the β-ether followed by, or accompanied by, cleavage of the ester to form the arylpropanol **1**, Fig. 2. γ-Acylation of the β-aryl ethers (**16** and **17**) alters the reaction kinetics such that β-aryl ether bond cleavage is preferred over hydrogenation of the carbocation. For compound **17**, the relative reaction rates shift to almost complete loss of the β-aryl ether and only trace detectable amount of compound **21′**.

Extending the reaction time does not result in higher levels of arylpropane **2** relative to arylpropanol **1**, indicating that arylpropane **2** derived from an intermediate on the reaction pathway and not from degradation of arylpropanol **1**. Previously we noted that treating corn stover (*Zea mays*) lignin with sodium hydroxide reduced the relative amount of arylpropane **2** vs arylpropanol **1**[25]. We interpreted this observation to indicate that the presence of the γ-acyl groups increased the apparent cleavage of the C_γ–O_γ bond, but we did not provide a mechanism for how this occurred. In Fig. 2 (Pathway A) we propose a mechanism for heterogenous palladium-catalyzed hydrogenolysis of acylated β-aryl ethers that produces the portfolio of products observed from model compound studies. Our mechanism is based on previously proposed homogenous palladium-catalyzed hydrogenolysis mechanisms[26].

Mechanisms of hydrogenolysis

Hydrogenolysis of biomass (or lignin) begins with the solvent-mediated extraction of the intact lignin polymer from the biomass (or lignin particle). As is typically described in organosolv pretreatment, there are some auto-depolymerization mechanisms that can occur at this stage that are typically catalyzed by acid[27,28]. The lignin dissolved in a good solvent will be extended like wet spaghetti, in a poor solvent it will compress into a bead, and in either case may diffuse through the solvent to the catalyst surface. Once on the palladium surface the depolymerization mechanism starts with cleavage of the C_α–OH bond to generate a benzylic carbocation, Fig. 2 Pathway A. This occurs either 1) By dissociation of the C_α–OH bond to generate a resonance-stabilized benzylic carbocation and a hydroxy anion (A_1), followed by coordination to the palladium surface (complex A_2), which further stabilizes the carbocation by forming a Pd(II)–C_α bond; or 2) With the β-aryl ether coordination to the palladium surface followed by Pd(0)-insertion (oxidative addition) across the benzylic C_α–OH bond to form Pd(II)–C_α and Pd(II)–OH bonds (complex A_2). The formation of the carbocation would be accelerated under acidic conditions, like those present in untreated biomass. Complex A_2 either reductively eliminates by reacting with a Pd(II)–H species to form the α-saturated β-aryl ether **27** and regenerate the Pd(0) surface; or complex A_2 undergoes β-phenoxy elimination to generate Pd(II)–**9** complex and the Pd(II)–OAr bond (A_3). The Pd(II)–OAr species then migrates across the Pd surface until encountering a Pd(II)–H species, at which point they reductively eliminate to form phenol **3** and regenerate the Pd(0) surface. The Pd(II)–**9** complex A_3 evolves temporally along two paths; 1) Dissociation from the surface, which results in the formation of reaction products from thermal decomposition of **9**, reactions with the solvent (transesterification and hydrolysis), and possibly later coordination back onto the palladium surface converts **9** to monolignol **25** and *p*-hydroxybenzoic acid **7** or the methyl ester **8**; or 2) Complex A_3 encounters a Pd(II)–H species, upon which the Pd(II)–H inserts across the $C_\alpha = C_\beta$ π-bond to generate the partially saturated Pd(II)-**9** species bound to the palladium surface through a Pd(II)–C_β bond (complex A_4). When complex A_4 encounters another Pd(II)–H species, a reductive elimination event occurs to regenerate the Pd(0) surface and form the observed compound **11**. Alternatively, complex A_4 can undergo Pd-assisted elimination of the allylic ester and generate propene derivative **10** and free acid **7**, a pathway known to be catalyzed by palladium[29]. Subsequent hydrogenation of propene **10** forms propane **2**.

Hydrogenolysis (reductive catalytic fractionation) of poplar wood

When poplar wood was treated under varying hydrogenolysis conditions (often referred to as reductive catalytic fractionation), the chromatographic peak for ester conjugate **11** was more prominent after short reaction times, Fig. 3a (EIC chromatogram insert for *m/z* 163). This product was previously reported to be present as a significant peak in the phenolic dimer fraction of poplar hydrogenolysis products[30]. Unlike the stable monomeric products that are typically reported in the literature (**1**, **2**, **8**, and truncated-sidechain products **3**–**5**) that continuously increase in abundance as the reaction progresses, the concentration of the semi-stable ester **11** increased under short reaction times (60 min) and then decreased in abundance as the reaction progressed (120 min and longer), Fig. 3b. Another pathway for ester **11** degradation was identified from an initially mysterious side-product (compound **14**, Figure 1 and Fig. 3a, with an $m/z = 352$ [$M_{11} + 20$], in which M_{11} is the molecular weight of ester **11**. We will explore the formation of this product in detail later in the discussion.

When arylpropanol esters **11** were subjected to the hydrogenolytic conditions, the major products were methyl ester **8**, arylpropanols **1**, and some arylpropanes **2**, the latter in a 4:1 area ratio for **1**:**2**, Fig. 1b and Supplementary Table 8, confirming that direct hydrogenolysis of the ester across the C_γ–O bond does not proceed efficiently. If the catalyst surface was hydrogen-limited, the half-life of the unsaturated monolignol conjugate intermediates **9** formed in the β-aryl ether elimination step would increase[26]. The longer half-life enables kinetically slower reaction pathways to become competitive with hydrogenation of the double bond, such as the Pd-assisted allylic ester elimination from complex A_4 to propene **10**. Hydrogenation of arylpropenes **10** to arylpropanes **2** would occur once the catalyst-bound hydrogen is replenished. Alternatively, monolignol conjugates **9** or arylpropenes **10** could react through palladium-catalyzed coupling reactions with MeOH (or other alcohols) to produce arylpropanol methyl ethers **6** (γ-OMe)[31–33]. In these scenarios, the amount of arylpropane **2** and methyl ether **6** would increase when the palladium surface became hydrogen deficient due to mass-transport limitations. In Supplementary Table 8, the amount of arylpropane **2** and ether **6** are equal (**2**:**6** = 1:1 by area), supporting a local environment deficient in the Pd–H species. Further evidence of these effects can be observed by the increase of unsaturated products formed in the high-throughput hydrogenolysis technique reported by Kenny et al. as compared to their classic batch-hydrogenolysis results[34].

Oxidation of *p*-hydroxybenzoate esters during hydrogenolysis

The GC-MS chromatograms associated with longer hydrogenolysis reaction times for poplar samples, Fig. 3a, showed a set of new

https://doi.org/10.1038/s41467-025-60270-x

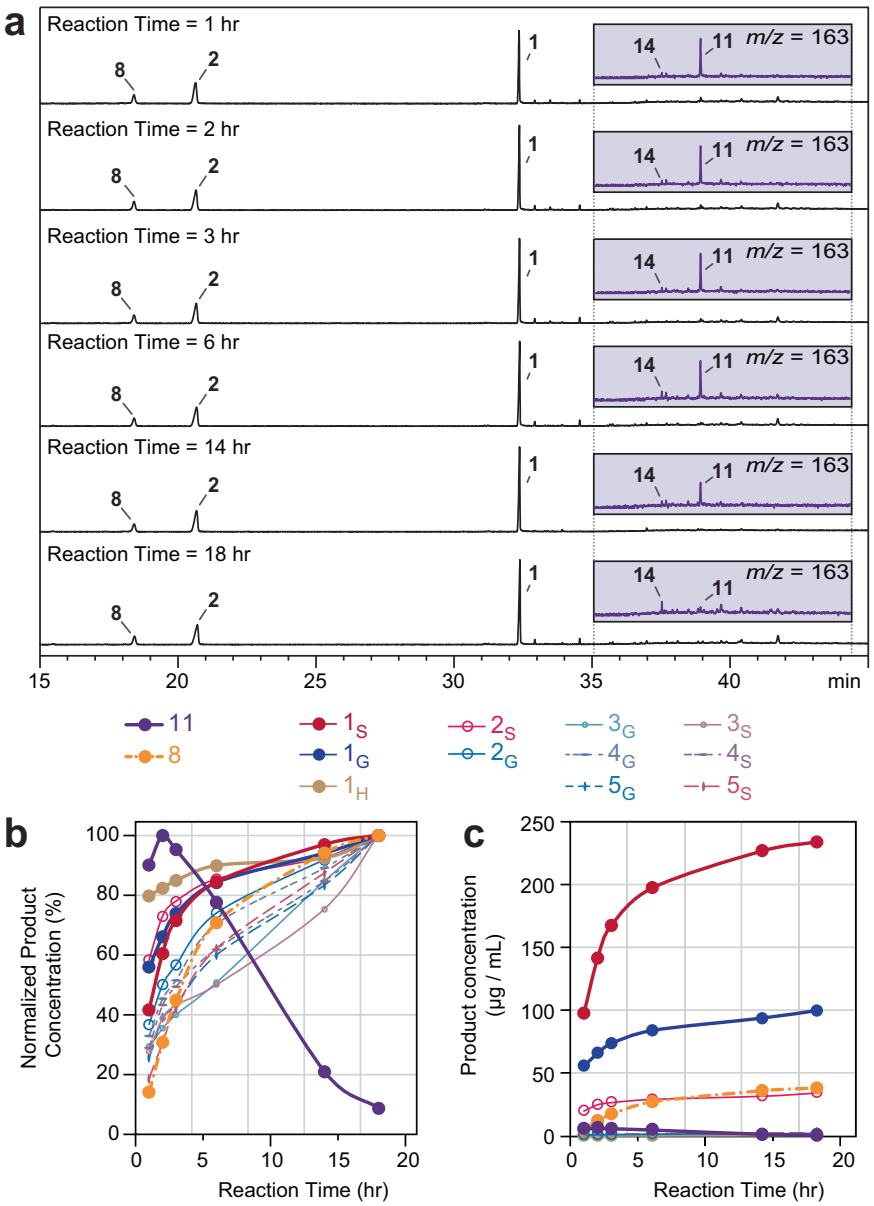

Fig. 3 | The reaction-time dependence of hydrogenolysis products from NM6 poplar as observed by GC-MS. a The GC-MS total-ion chromatograms (TIC) of NM6-poplar hydrogenolysis products as a function of reaction time. Inserts show the extracted-ion chromatograms (EIC) for the $[eugenol\text{-}H]^+$ fragment ion $m/z = 163$, as the reaction time increases the abundance of product **11** decreases in intensity compared to product **14**. **b** The time evolution of each monitored phenolic product normalized to the maximum observed concentration. **c** The quantified amount of monitored phenolic product vs. reaction time. The key for plots **b** and **c** are color, symbol, and line style coded by compound, with the G denoting a guaiacyl based unit and S denoting a syringyl based unit.

peaks with $m/z = 338$ [$M_{11} + 6$], 348 [$M_{11} + 16$], 350 [$M_{11} + 18$], and 352 [$M_{11} + 20$], in which M_{11} is the molecular weight of ester **11**. The mass-fragmentation patterns of these peaks indicated the retention of arylpropanol **1** subunit and a loss of the intact *p*-hydroxybenzoate moiety. HPLC isolation of the [$M_{11} + 20$] product followed by 2D NMR characterization for structural identification indicated the addition of a 2-hydroxy group to the *p*-hydroxybenzoate ring to generate 2,4-dihydroxybenzoate ester **13**, Fig. 1, that underwent partial saturation while still retaining the ester linkage to arylpropanol **1**, to produce the observed [$M_{11} + 20$] product **14**, Fig. 4a. Under similar reaction conditions, palladium has been reported to perform carbonyl-assisted C–H bond activation *ortho* to carboxylate groups of aromatic compounds[35–37]. In the proposed mechanism for hydrogenolysis of β-aryl ethers, there would be surface-bound hydroxy groups (possibly from the benzylic C_α–OH bond insertion step or from water in the methanol solvent), and a deficiency in local Pd–H availability (indicated by the formation of arylpropane **2** or methyl ether **6**). Temporally, the typically reductive catalyst surface conditions could therefore be primed for oxidative addition of a hydroxy group to the *p*-hydroxybenzoate ester, *ortho* to the carboxylate, to form the 2,4-dihydroxybenzoate ester **13**. Once the surface-bound Pd–H is replenished, the catalyst continues derivatizing the intermediate by hydrogenation of the 2,4-dihydroxybenzoate ester to the partially saturated 2,4-dihydroxy-cyclohex-1-enoate ester **14**. The stepwise nature of this reaction is deduced from the presence of dihydroxybenzoate **13**, followed by sequential hydrogenation to products with $m/z = [M_{11} + 16]$, [$M_{11} + 18$], and [$M_{11} + 20$]. When the local environment is not hydride-deficient or lacks Pd–OH, some ester **11** is reduced to the arylpropyl 4-hydroxy-cyclohexanoates **12**.

https://doi.org/10.1038/s41467-025-60270-x

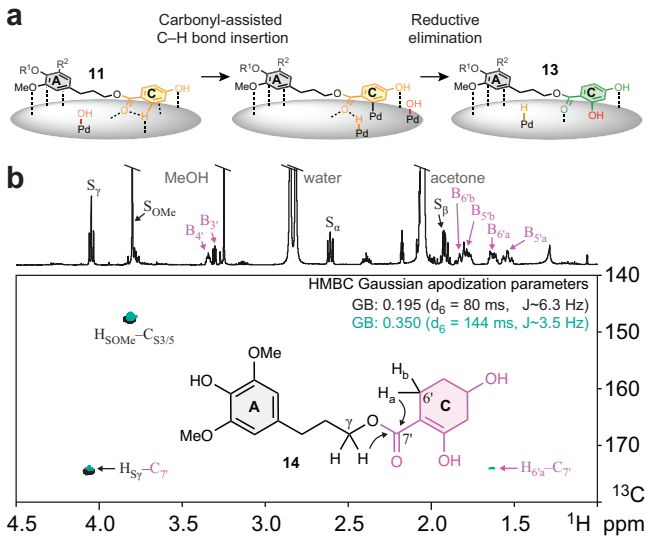

Fig. 4 | The oxidized and reduced [M_{11} + 20] product isolated by HPLC purification of the crude product mixture produced by treating ester 11 in methanol at 200 °C, under 30 bar H_2 in the presence of Pd/C. a A proposed mechanism for carbonyl-assisted Pd-catalyzed C–H bond activation and subsequent oxidation of the *p*-hydroxybenzoate subunit (yellow) to 2,4-dihydroxybenzoate (green) to give product **13**, Fig. 1, the added hydroxy group is in red. **b** 2D HMBC NMR spectra (in acetone-d_6) of isolated compound **14** showing, overlapped, the signals from spectra processed via Gaussian apodization to optimize for long-range couplings of ~6 Hz (black) and ~3 Hz (teal) of the 2,4-dihydroxy-cyclohex-1-enonate's carbonyl carbon ($C_{7'}$) to the γ-hydrogen of the 3-(syringyl)propyl moiety and $C_{7'}$ to the $H_{6'a}$ of the 2,4-dihydroxy-cyclohex-1-enonate moiety.

Previous work on combining oxidative Pd-catalyzed C–H bond activation with hydrogenation using the same catalyst under one set of reaction conditions required specifically designed setups that used controlled membrane reactors to supply hydrogen gas to the system[35,36]. Here we show that the high demand for catalyst-bound hydrogen to perform the sequential hydrogenolytic steps in the cleavage of β-ethers provides a temporal window for oxidative processes to occur while the compound is still bound to the catalyst's surface. As hydrogenolysis has utilized many transition metal catalysts that are also often used for other chemical transformations (e.g., oxidative C–C-bond-forming reactions)[38], the phenolic monomer pool that is currently understood from hydrogenolysis has been somewhat undercharacterized. This has impacts on the quantification of depolymerization yields for downstream utilization of the product mixture for microbial funneling, modeling product isolation, and reaction condition optimization. The observations here also open the door to designing catalysts to produce more complex chemical products for advanced materials applications than could be envisioned by stepwise reductive or oxidative catalytic processes.

Discussion

In this study, we show that hydrogenolysis of naturally γ-acylated lignins using Pd/C in methanol cleaves the β-ether bonds and releases saturated arylpropyl esters that subsequently degrade to arylpropanols and the methyl esters or free acid from the acyl moiety. Optimization catalytic lignin depolymerization requires an accounting of products that retain the γ-acyl group. Many of the attempts to optimize the process do not consider non-catalytic decomposition of reaction intermediates, such as the arylpropyl esters **11** reported here and their transesterification to arylpropanols **1** and ester **8** (or acid **7**). Knowing that such ester bonds are semi-stable under hydrogenolytic reaction conditions provides researchers with a new set of variables to consider for targeting the conservation or degradation of these species.

The carbonyl assisted Pd-catalyzed C-H bond activation to oxidize arylpropyl ester **11** between reductive hydrogenolysis of the β-ether bond and a series of hydrogenation steps, provides a template for designing complex reaction pathways. The key is temporally controlling the local surface environment of the catalyst and availability of both oxidative (Pd-OH) and reductive (Pd-H) species. This template can be used to set-up cascading multi-catalytic step reaction sequences that uses one heterogenous catalytic surface and include both reductive and oxidative steps.

Methods

Chemicals

All commercially available chemicals were purchased from Millipore Sigma (St Louis, MO), Fisher Scientific (Chicago, IL), VWR (Batavia, IL), TCI America (Portland, OR), Acros International (Livingston, NJ), Neta scientific (Hainesport, NJ), and Ambeed (Arlington Heights, IL). Specialty gasses (i.e., hydrogen, argon, and helium) were purchased from Airgas (Madison, WI). The palladium on carbon (Pd/C) catalyst used in this study was 5 wt% palladium on a matrix of activated carbon support (Millipore Sigma P/N: 205680). The catalyst was used as received.

Biomass

The NM6 hybrid poplar (*Populus maximowiczii* × *nigra*) was produced by the Great Lakes Bioenergy Research Center and used in previous studies[39,40]. The poplar was debarked, chipped, dried, and fractionated to pass through a 5 mm round hole on a shaker table. The chips were then further milled to a fine powder with a Retsch MM400 shaker mill. Approximately ~2 g were loaded into a 50 mL stainless steel jar along with one 25 mm stainless-steel ball-bearing, and the samples milled at 30 Hz for 5 min.

Hydrogenolysis of biomass (reductive catalytic fractionation)

The NM6 poplar was treated by hydrogenolysis using hydrogen over a palladium on carbon (5 wt% Pd/C) catalyst in MeOH. In a 50 mL Hastelloy Parr reactor, equipped with a mechanical stirrer and heating mantle, 750 mg of biomass, 75 mg Pd/C, 30 mL MeOH, and 9 mg (65 μmol) 1,2-dimethoxybenzene (DMB, an internal standard for determining monomer yields) were added. The reactor was sealed, purged, and pressurized with hydrogen gas up to 30 bar. The reaction vessel was then heated to 200 °C and held there for 1-18 h (200 °C, 60 bar). Following reaction, the heating mantle was removed, and the reactor was rapidly cooled to room temperature at which point the reaction vessel was depressurized. The catalyst and any residual solids were removed by filtration through a 1 μm PTFE (polytetrafluoroethylene) filter. The product mixture's composition was measured by GC-MS, see Supplemental Information.

Hydrogenolysis of model compounds

The model compounds were treated by hydrogenolysis using hydrogen over 5 wt% Pd/C catalyst in MeOH. In a 50 mL Hastelloy Parr reactor, equipped with a mechanical stirrer and heating mantle, 10-30 mg of the model compound, 5–15 mg Pd/C, and 30 mL MeOH were added. The reactor was sealed, purged, and pressurized with hydrogen gas up to 30 bar. The reaction vessel was then heated to 200 °C and held there for 3 h (200 °C, 60 bar). Following reaction, the heating mantle was removed, and the reactor was rapidly cooled to room temperature at which point the reaction vessel was depressurized. The catalyst was removed by filtration through a 1 μm PTFE (polytetrafluoroethylene) filter. The product mixture was directly injected into a GC-MS for product compositional analysis and a LC-PDA to determine the percent conversion of β-aryl ether models, see Supplemental Information.

Synthesis of model compounds

γ-Acylated-β-aryl ether model compounds **15** and **17** (Fig. 1) were prepared from acetovanillone and acetosyringone, respectively, following a previously reported synthetic scheme[22]. 4-*O*-Methyl analogs **16** and **18**, used to model internal units, were prepared from internal β-aryl ether models with 4-*O*-methylation on the "A" ring, following the same synthetic strategy[41–43]; see Supplemental Information for synthetic details. Compounds **11**, **12**, **13**, and **19'** were synthesized as described in the Supplemental Information using previously published protocols where available[44–47].

Data availability

The authors declare that the data supporting the findings of this study are available within the article and its Supplementary information files.

References

1. Sun, Z., Fridrich, B., de Santi, A., Elangovan, S. & Barta, K. Bright side of lignin depolymerization: Toward new platform chemicals. *Chem. Rev.* **118**, 614–678 (2018).
2. Schutyser, W. et al. Chemicals from lignin: an interplay of lignocellulose fractionation, depolymerisation, and upgrading. *Chem. Soc. Rev.* **47**, 852–908 (2018).
3. Li, Y. et al. Mechanistic study of diaryl ether bond cleavage during palladium-catalyzed lignin hydrogenolysis. *ChemSusChem* **13**, 4487–4494 (2020).
4. Parthasarathi, R., Romero, R. A., Redondo, A. & Gnanakaran, S. Theoretical study of the remarkably diverse linkages in lignin. *J. Phys. Chem. Lett.* **2**, 2660–2666 (2011).
5. Huang, J.-B. et al. Theoretical study of bond dissociation energies for lignin model compounds. *J. Fuel Chem. Technol.* **43**, 429–436 (2015).
6. Li, C. Z., Zhao, X. C., Wang, A. Q., Huber, G. W. & Zhang, T. Catalytic transformation of lignin for the production of chemicals and fuels. *Chem. Rev.* **115**, 11559–11624 (2015).
7. Kumaniaev, I. et al. Lignin depolymerization to monophenolic compounds in a flow-through system. *Green. Chem.* **19**, 5767–5771 (2017).
8. De Santi, A. et al. New mechanistic insights into the lignin beta-O-4 linkage acidolysis with ethylene glycol stabilization aided by multilevel computational chemistry. *ACS Sustain. Chem. Eng.* **9**, 2388–2399 (2021).
9. Smith D. C. C. *p*-Hydroxybenzoate groups in the lignin of aspen (*Populus tremula*). *J. Chem. Soc.* 2347–2351 https://doi.org/10.1039/JR9550002347 (1955).
10. Pearl, I. A., Beyer, D. L. & Laskowski, D. Alkaline hydrolysis of representative palms. *TAPPI* **42**, 779–782 (1959).
11. Hartley, R. D. & Harris, P. J. Phenolic constituents of the cell walls of dicotyledons. *Biochem. Syst. Ecol.* **9**, 189–203 (1981).
12. Harris, P. J. & Hartley, R. D. Phenolic constituents of the cell walls of monocotyledons. *Biochem. Syst. Ecol.* **8**, 153–160 (1980).
13. Karlen, S. D. et al. Commelinid monocotyledon lignins are acylated by *p*-coumarate. *Plant Physiol.* **177**, 513–521 (2018).
14. de Vries, L. et al. *p*HBMT1, a BAHD-family monolignol acyltransferase, mediates lignin acylation in poplar. *Plant Physiol.* **188**, 1014–1027 (2022).
15. Goacher, R. E., Mottiar, Y. & Mansfield, S. D. ToF-SIMS imaging reveals that *p*-hydroxybenzoate groups specifically decorate the lignin of fibres in the xylem of poplar and willow. *Holzforschung* **75**, 452–462 (2021).
16. Lu, F. & Ralph, J. Novel tetrahydrofuran structures derived from β–β-coupling reactions involving sinapyl acetate in Kenaf lignins. *Org. Biomol. Chem.* **6**, 3681–3694 (2008).
17. Lu, F., Ralph, J. Preliminary evidence for sinapyl acetate as a lignin monomer in kenaf. *J. Chem. Soc. Chem. Commun.* 90–91 https://doi.org/10.1039/B109876D (2002).
18. Hatfield, R. D. et al. Grass lignin acylation: *p*-coumaroyl transferase activity and cell wall characteristics of C3 and C4 grasses. *Planta* **229**, 1253–1267 (2009).
19. Withers, S. et al. Identification of a grass-specific enzyme that acylates monolignols with *p*-coumarate. *J. Biol. Chem.* **287**, 8347–8355 (2012).
20. Petrik, D. L. et al. *p*-Coumaroyl-CoA:Monolignol Transferase (PMT) acts specifically in the lignin biosynthetic pathway in *Brachypodium distachyon*. *Plant J.* **77**, 713–726 (2014).
21. Zhao, Y. et al. Monolignol acyltransferase for lignin *p*-hydroxybenzoylation in *Populus*. *Nat. Plants* **7**, 1288–1300 (2021).
22. Lu, F. et al. Naturally *p*-hydroxybenzoylated lignins in palms. *BioEnergy Res.* **8**, 934–952 (2015).
23. Li, H. & Song, G. Paving the way for the lignin hydrogenolysis mechanism by deuterium-incorporated β-O-4 mimics. *ACS Catal.* **10**, 12229–12238 (2020).
24. Li, Y. et al. Kinetic and mechanistic insights into hydrogenolysis of lignin to monomers in a continuous flow reactor. *Green. Chem.* **21**, 3561–3572 (2019).
25. Timokhin, V. I. et al. Production of *p*-coumaric acid from corn GVL-lignin. *ACS Sustain. Chem. Eng.* **8**, 17427–17438 (2020).
26. Grossman, R. B. *The art of writing reasonable organic reaction mechanisms*. (Springer, New York, ed. 2nd, 2003), pp. xvi, 355 p.
27. Joseph, P., Ottesen, V., Opedal, M. T. & Moe, S. T. Morphology of lignin structures on fiber surfaces after organosolv pretreatment. *Biopolymers* **113**, e23520 (2022).
28. Bujanovic, B. et al. Use of renewable alcohols in autocatalytic production of aspen organosolv lignins. *ACS Omega* **9**, 38227–38247 (2024).
29. Tsuji, J., Minami, I. & Shimizu, I. Preparation of 1-alkenes by the palladium-catalyzed hydrogenolysis of terminal allylic carbonates and acetates with formic-acid triethylamine. *Synthesis* **1986**, 623–627 (1986).
30. Renders, T. et al. Influence of acidic (H_3PO_4) and alkaline (NaOH) additives on the catalytic reductive fractionation of lignocellulose. *ACS Catal.* **6**, 2055–2066 (2016).
31. Hosokawa, T., Ohta, T., Kanayama, S. & Murahashi, S. I. Palladium(II)-catalyzed acetalization of terminal olefins bearing electron-withdrawing substituents with optically-active diols. *J. Org. Chem.* **52**, 1758–1764 (1987).
32. Fernandes, R. A., Chandra, N., Gangani, A. J. & Khatun, G. N. Palladium-catalyzed regioselective intermolecular hydroalkoxylation of 1-arylbutadienes. *J. Org. Chem.* **88**, 10339–10354 (2023).
33. Haight, A. R., Stoner, E. J., Peterson, M. J. & Grover, V. K. General method for the palladium-catalyzed allylation of aliphatic alcohols. *J. Org. Chem.* **68**, 8092–8096 (2003).
34. Kenny, J. K. et al. Design and validation of a high-throughput reductive catalytic fractionation method. *JACS Au* **4**, 2173–2187 (2024).
35. Sato, K. et al. Direct hydroxylation of aromatic compounds by a palladium membrane reactor. *Catal. Today* **104**, 260–266 (2005).
36. Sato, K. et al. Direct hydroxylation of methyl benzoate to methyl salicylate by using new Pd membrane reactor. *Catal. Lett.* **96**, 107–112 (2004).
37. Dutta, S. et al. Pd-catalysed C–H functionalisation of free carboxylic acids. *Chem. Sci.* **13**, 2551–2573 (2022).
38. Iretskii, A. V., Sherman, S. C., White, M. G., Kenvin, J. C. & Schiraldi, D. A. The oxidative coupling of methyl benzoate. *J. Catal.* **193**, 49–57 (2000).
39. Perez, J. M. et al. Integrating lignin depolymerization with microbial funneling processes using agronomically relevant feedstocks. *Green. Chem.* **24**, 2795–2811 (2022).
40. Pastore de Lima, A. E. et al. On the synthesis of biorefineries for high-yield isobutanol production: from biomass-to-alcohol experiments to system level analysis. *RSC Sustain.* **2**, 2532–2540 (2024).

41. Picart, P. et al. From gene towards selective biomass valorization: Bacterial β-etherases with catalytic activity on lignin-like polymers. *ChemSusChem* **7**, 3164–3171 (2014).
42. Teske, J. & Plietker, B. Fe-catalyzed cycloisomerization of aryl allenyl ketones: Access to 3-arylidene-indan-1-ones. *Org. Lett.* **20**, 2257–2260 (2018).
43. Lancefield, C. S., Ojo, O. S., Tran, F. & Westwood, N. J. Isolation of functionalized phenolic monomers through selective oxidation and C–O bond cleavage of the β-O-4 linkages in lignin. *Angew. Chem. (Int. Ed.)* **54**, 258–262 (2015).
44. Zhu, Y. et al. Preparation of monolignol γ-acetate, γ-*p*-hydroxycinnamate, and γ-*p*-hydroxybenzoate conjugates: Selective deacylation of phenolic acetates with hydrazine acetate. *RSC Adv.* **3**, 21964–21971 (2013).
45. Regner, M., Bartuce, A., Padmakshan, D., Ralph, J. & Karlen, S. D. Reductive cleavage method for quantitation of monolignols and low-abundance monolignol conjugates. *ChemSusChem* **11**, 1600–1605 (2018).
46. Boschi, D. et al. NO-donor phenols: a new class of products endowed with antioxidant and vasodilator properties. *J. Med. Chem.* **49**, 2886–2897 (2006).
47. Sadler, J. C., Chung, C.-W. H., Mosley, J. E., Burley, G. A. & Humphreys, L. D. Structural and functional basis of C-methylation of coumarin scaffolds by NovO. *ACS Chem. Biol.* **12**, 374–379 (2017).

Acknowledgements

This work was supported by the U.S. Department of Energy (DOE) Great Lakes Bioenergy Research Center (DOE Office of Science BER grant no. DE-SC0018409, Timothy J. Donohue, C. S., V. T., J. H., J. R. and S. K.) and the Swiss National Science Foundation (Sinergia) grant # CRS115_180258, J. R. and C. S.

Author contributions

C. S., J. R. and S. K. conceptualized the project; C. S. and S. K. performed the investigation; V. T., J. H. and S. K. synthesized the model compounds; C. S., J. R., V.T. and S. K. analyzed the data; C. S. and S. K. wrote the manuscript; all authors contributed to the editing of the manuscript.

Competing interests

The authors declare no competing interests.

Additional information

Supplementary information The online version contains supplementary material available at https://doi.org/10.1038/s41467-025-60270-x.

Correspondence and requests for materials should be addressed to Steven D. Karlen.

Peer review information *Nature Communications* thanks the anonymous reviewers for their contribution to the peer review of this work. A peer review file is available.